Sediment oxygen uptake and hypoxia: a simple mass-balance model for estuaries and coastal oceans

Jing Sun[1,2], Liuqian Yu[2,3]*, Xingyu Yang[1,2], Jianping Gan[1,2], Hongbin Yin[4], and Jiying Li[1,2]*

[1]Department of Ocean Science, The Hong Kong University of Science and Technology, Clear Water Bay, Kowloon, Hong Kong SAC, P. R. China

[2]Center for Ocean Research in Hong Kong and Macau, Hong Kong SAC, P. R. China

[3]Earth, Ocean and Atmospheric Sciences Thrust, The Hong Kong University of Science and Technology (Guangzhou), Guangdong, P.R. China

[4]Nanjing Institute of Geography and Limnology, Chinese Academy of Science, Nanjing, Jiangsu, P. R. China

Corresponding author:
Jiying Li (jiyingli@ust.hk; OCRID: 0000-0003-1677-6922)
Liuqian Yu (liuqianyu@hkust-gz.edu.cn; OCRID: 0000-0002-5492-8213)

Key Points:

- Sediment respires >60% of the organic matter produced in the water column of the Pearl River Estuary (PRE) region, leading to high sediment oxygen uptake.
- The sediment's effect on the bottom oxygen loss is controlled by the thickness of the bottom boundary layer.
- We develop a simple and generic mass-balance model to understand hypoxia conditions and timescales in the PRE and similar coastal systems.

Abstract

Hypoxia is increasing in coastal oceans. This is because eutrophication has increased oxygen consumption, while less oxygen is replenished to the bottom under stronger stratification. Quantifying these biogeochemical and physical drivers is important for management and predicting future trends. By using observations from the Pearl River Estuary (PRE) region (10-70 m deep) and similar coastal systems, this paper introduces a simple analysis to quantify both the biogeochemical and physical drivers of hypoxia. We show that in the PRE region, sediment respires >60% of organic matter produced in the water column, leading to high sediment oxygen uptake (average 41.1±16.3 mmol m^{-2} d^{-1}) and shallow oxygen penetrations (2-7 mm). The sediment's effect on the bottom oxygen loss becomes stronger with the reducing thickness of the bottom boundary layer. We then construct a generic mass-balance model to quantify oxygen loss, determine timescales of hypoxia formation, and explain within- and cross-system variabilities.

Plain language summary

Coastal oceans, especially those off rivers and estuaries, frequently experience low-oxygen conditions such as hypoxia (dissolved O_2 < 2 mg L^{-1}). This is because the nutrient-rich coastal ocean produces high amount of organic matter, which settles to the bottom waters to consume oxygen. Hypoxia becomes more severe if the resupply of oxygen from the atmosphere and the surface water to the bottom water is blocked by strong density stratification. To quantify these effects, we study a typical coastal system, the Pearl River Estuary and the adjacent shelf, combining field and lab observations and mass-balance modeling. We find that sediment consumes a substantial amount of oxygen, and its contribution to hypoxia can be predicted if we know how thick the stratified bottom layer is. We derive some simple equations to understand oxygen loss, which can tell us what level of oxygen consumption can render the system hypoxia, and for how long the stratification needs to be maintained for hypoxia to develop. We also show that the model is generic and can be applied to other similar coastal systems, such as the northern Gulf of Mexico and the Changjiang Estuary region, to explain the variability in hypoxia conditions and timescales.

1 Introduction

Low oxygen conditions are becoming more frequent in coastal oceans, affecting biogeochemical cycles and marine life (Katsev et al., 2007; Levin et al., 2009; Middelburg & Levin, 2009). These conditions are a result of high oxygen consumption and weak ventilation, especially in bottom waters where oxygen depletion can be severe, leading to hypoxia (O_2 < 2 mg L^{-1}). In estuaries and coastal shelves, oxygen is rapidly consumed due to the high organic matter production driven by terrestrial and/or upwelling nutrients; freshwater inputs also enhance vertical density stratification and reduce the oxygen resupply to the bottom. The increasing anthropogenic fertilization of the coastal ocean, together with the stronger stratification caused by global warming, therefore, can intensify hypoxia in both magnitude and duration (Diaz & Rosenberg, 2008).

Quantifying these physical and biogeochemical drivers of hypoxia is important for management and predicting future trends. In addition to monitoring oxygen (Grégoire et al., 2021), mechanistic modeling becomes very useful (Laurent & Fennel, 2017; Peña et al., 2010). These models simulate the oxygen budget considering its source/sink components, including physical transports, air-sea exchanges, photosynthesis, and biogeochemical consumption in the water column and sediments (Peña et al., 2010; Testa et al., 2017). Among models of various complexity, coupled-physical-biogeochemical models are the most comprehensive, for they simulate the interactions between nutrient-driven organic matter productivity and physical transport, the two major drivers of oxygen variability (Fennel et al., 2016; Yu et al., 2015a, 2021). These models, however, rely on parametrizations of many processes, for example, the relationships between lights, temperature, nutrients, organic matter production, respiration, food-web dynamics, and the reactions in the sediments and benthic-pelagic exchanges (Peña et al., 2010; Yu et al., 2015a, b, 2021). Moreover, parametrizations can be system-specific and need to be well constrained by a large matrix of observations (e.g., dynamics in biomass indicators, nutrients, and physical properties). Thus, the models usually have low transferability among systems (Peña et al., 2010). For cross-system comparison, simple scale analyses are useful (Fennel & Testa, 2019). For example, the vulnerability of the system can be understood by comparing the timescale of hypoxia formation to the water residence time of the region (Fennel & Testa, 2019). However, while such an approach provides regional order-of-magnitude understanding, it is inadequate for describing local heterogeneity, which is important for estuarine coastal systems.

This paper introduces a simple analysis that can describe regional heterogeneity and also enables cross-system comparison. By using water column and sediment oxygen data across a typical estuary and coastal shelf, we derive a simple mass-balance model to understand oxygen loss without a detailed formulation of the physical and biogeochemical complexity. The model can be used to understand the sensitivity of the system to both the biogeochemical and physical drivers of hypoxia. We then discuss how the model can be generalized to understand within-and cross-system variability,

using examples from similar coastal systems including the Northern Gulf of Mexico, the Changjiang Estuary region, and the Chesapeake Bay.

2. Field Methods

We study the Pearl River Estuary and adjacent shelf waters (PRE region) in the summer of 2021 (Fig.1a and Table.S1; Li et al. 2024). We used a SeaBird-SBE17-plus conductivity–temperature–depth (CTD) to measure the water column temperature, density, salinity, O_2 concentrations and calculated the buoyancy frequency (N^2; s^{-2}):

$$N^2 = \frac{g}{\rho(z)}\frac{d\rho(z)}{dz} \qquad \text{Eq.1}$$

g is gravity acceleration; z is water depth; ρ is potential density. High N^2 means high stability of the water column.

Sediment cores with undisturbed overlying waters were collected using a Uwitec corer. Oxygen micro-profiles were obtained using a Unisense O_2 electrode. The sediment-water interface has the sharpest oxygen gradient. Oxygen penetration depth was defined as the depth where oxygen is under the detection limit of ~0.3 μmol L^{-1}. Total sediment oxygen uptake (SOU; mmol m^{-2} d^{-1}), defined as the downward flux of oxygen into the sediment, was determined using onboard whole-core incubations: sediment cores were stabilized, sealed, and monitored for the oxygen concentrations in the overlying waters, which were gently stirred to generate the water movement and create a diffusive boundary layer (Bowman & Delfino, 1980; Glud, 2008). SOU was calculated from the linear decrease of oxygen. The incubation typically lasts 2-3 hours. Detailed methods are described in SI.1.

3. Results

3.1 Stratification and hypoxia in the water column – The water column develops hypoxia within the nearshore waters (10-20 m) off the estuary during the summer (Fig.1a), whereas offshore sites (>30 m) are well oxygenated. Such local seasonal hypoxia has been observed for several recent years (Li et al., 2020; Yu et al., 2021). At most sites, the water column is stratified by vertical gradients of temperature and salinity (Figs.1b and S1): the surface water from the upstream is warmer and fresher, while the bottom seawater is colder and saltier. In the stratified waters, the surface mixed layers are thin, with the density drastically increasing below 5-10 m forming a pycnocline (Fig.S1). This parallels the changes of buoyancy frequency (N^2) (Fig.1c), which peaks within the pycnocline and decreases downward, until the density has little variation, forming a stable bottom boundary layer (BBL; Figs.1c and S1) (Trowbridge & Lentz, 2018). We defined the upper boundary of BBL as the depth where N^2 increases drastically above (i.e., $N^2 > 0.01$ s^{-2}). The BBL has homogenously lower oxygen and reaches hypoxia at some sites (Figs.1a and 1c).

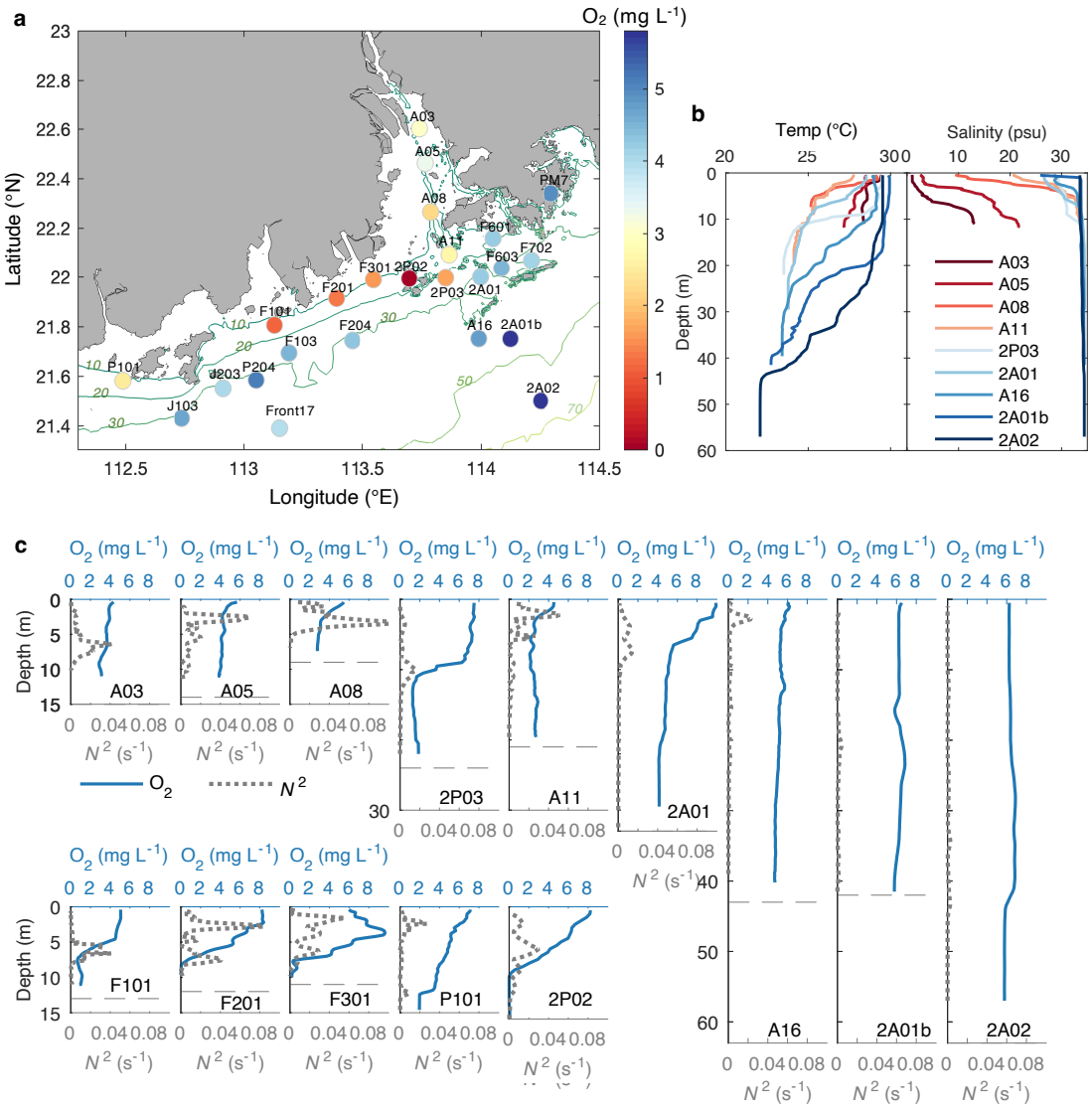

Figure 1 Water column physiochemistry in the Pearl River Estuary region. a) *Sampling locations and bottom oxygen concentrations;* ***b****) Temperature and salinity profiles across the estuary to open ocean gradient* ***c****) Buoyancy frequency (N^2) and O_2 profiles across the salinity gradient and at the hypoxic sites. Horizontal dashed lines represent the bottom.*

3.2 Sediment oxygen uptake and bottom water oxygen – Oxygen concentration in the BBL is controlled by the flux from the upper layer, which can be restricted by stratification, and the consumption in the water and sediments. In the sediments, oxygen drops sharply from 75-150 μmol L^{-1} near the interface to nondetectable (<0.3 μmol L^{-1}) within a few millimeters downcore (1-7 mm; Figs.2a and S3). Oxygen penetration decreases with decreasing water depths, consistent with global observations but more dramatically compared to the open ocean (Figs. S4b and S4c). The drastic depletion of oxygen in sediments is a result of high SOU (16.5-70.5 mmol m^{-2} d^{-1}, average 41.1±16.3

mmol m^{-2} d^{-1}; Fig.2b and Table.S1), consistent with typical coastal sediments (Fig.S4d). Nearshore sediments have relatively higher SOU compared to offshore (Fig.2b). If we assume oxygen is predominantly consumed via organic matter respiration, this consumption averages to ~62±25% of the organic matter produced in the water column of the region (66 mmol m^{-2} d^{-1}) (Cai et al., 2004).

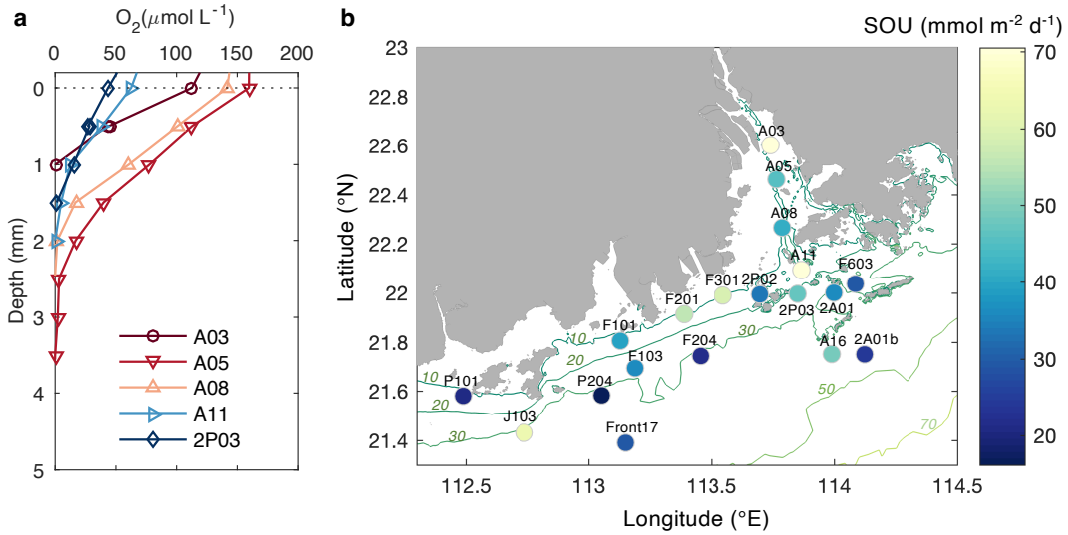

Figure 2 Sediment oxygen distribution and uptake. a) *O_2 profiles at selected sites;* ***b)*** *sediment oxygen uptake (SOU).*

High SOU would contribute significantly to the oxygen loss in the bottom water. However, the correlation between SOU and bottom oxygen is weak (Fig.S5 and Yu et al. (2015a)). This is because the thickness of the BBL would affect the sediment's impact: a thin layer would respond faster to SOU, while a thicker bottom reacts less with the effect of SOU being diluted. Indeed, the hypoxia sites have thin BBL (1.3 to <10 m), whereas the well-oxygenated sites have thicker BBL or entirely mixed water column (Figs.1c, S2, and Table.S1). By normalizing SOU to the thickness of the BBL (*h*), we obtain the oxygen depletion rate in the BBL by the sediments (SOU/*h*; mmol m^{-3} d^{-1}), which exhibits a strong relationship with the bottom O_2 level (Fig.3a). A stronger correlation appears when considering the integrated O_2 over the BBL (mmol m^{-2}): oxygen decreases exponentially with increasing SOU/*h* (Fig.3b). The relationships exist in similar systems such as the northern Gulf of Mexico and the Changjiang Estuary region (Figs.3a and 3b); both are estuary dominated shelves experiencing hypoxia (McCarthy et al., 2013; Zhu et al. 2016).). Similar relationships are also seen for the entire water column (Fig.S6).

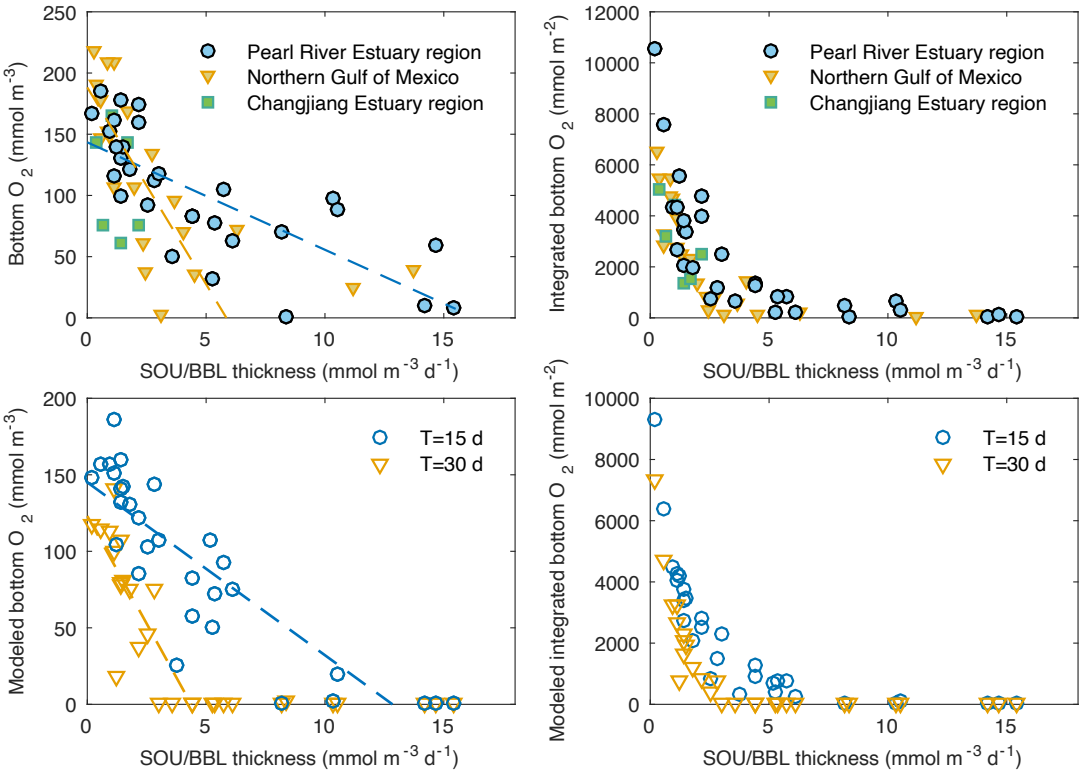

Figure 3 Bottom oxygen vs SOU normalized to BBL thickness (SOU/h). a *and* ***b)*** *Bottom oxygen vs SOU/h in the PRE region, North Gulf of Mexico* (McCarthy et al., 2013)*, and Changjiang Estuary region* (Zhang et al., 2017)*;* ***c*** *and* ***d)*** *Modeled bottom oxygen vs SOU/h, using water stability periods of T= 15 and 30 days.*

The water column oxygen uptake (WOU) is not explicitly considered, but it does not mean WOU is not important and omitted. Instead, the robust relationships suggest an intrinsic connection between SOU and WOU, which are both driven by the degradation of organic matter. Their proportions are determined by the water thickness, which determines the time settling particles spend in the water and thus their leftovers to drive SOU. This explains the curvature in Fig.3b: at the sites with low SOU/*h*, the BBL is thick and thus WOU becomes important, making the oxygen level sensitive to the apparent per-SOU change (steeper slopes at low SOU/*h* in Figs.3b).

The strong correlations between oxygen level and SOU/*h* also suggest the possibility of parameterizing SOU. SOU is important in controlling the water column oxygen budget and sediment geochemistry and fluxes and rates (e.g., denitrification, sulfate reduction) (Li et al., 2018a, b; Li & Katsev, 2014), but published SOC data is scarce due to measurement challenges. The potential parameterization of SOU using more obtainable water column CTD data is useful.

4. The Mass-Balance Model — Inspired by the observations above, we construct a mass-balance model to explore their physical meanings and quantitative insights. Details

of the model are narrated in SI.2, which we briefly introduce here to facilitate discussion. The change of O_2 concentration in the BBL is caused by fluxes from above (assumed to be small and neglected here due to the large N_2 above the BBL) and the sediment ($F_{\text{s-O2}}$, which equals –SOU), and the reaction within the BBL ($F_{\text{BBL-O2}}$, which equals –WOU_{BBL}):

$$\frac{\mathrm{d}\bar{C}_{\text{BBL-O2}}}{\mathrm{d}t} = \frac{F_{\text{s-O2}}}{h} + \frac{F_{\text{BBL-O2}}}{h} \qquad \text{Eq.2}$$

Here, $\bar{C}_{\text{BBL-O2}}$ is the average O_2 concentration in the BBL. Assuming oxygen is mostly consumed to respire organic matter (Zhang & Li, 2010), $F_{\text{BBL-O2}}$ depends on the amount of organic carbon settling into the BBL ($C_{\text{w-C}}^{H-h}$; H is the total depth and h is the thickness of the BBL, hence the upper boundary of BBL is at H-h; the subscript 'w-C' stands for water-column carbon), the reaction rate (k_{w}), and the time the particles spend in the BBL (t=h/u_{w}; u_{w} is the particle settling velocity). Considering a 1C:1O_2 ratio and first-order reaction for simplicity, the reaction in the BBL is

$$F_{\text{BBL-O2}} = \int_{H-h}^{H} -k_{\text{w}} C_{\text{w-C}}\,\mathrm{d}z_{\text{w}} = \int_{H-h}^{H} -k_{\text{w}} C_{\text{w-C}}^{H-h} e^{-\frac{k_{\text{w}}}{u_{\text{w}}}(z_{\text{w}}-H+h)}\,\mathrm{d}z_{\text{w}} = u_{\text{w}} C_{\text{C}}^{H-h}\left(e^{-\frac{k_{\text{w}}}{u_{\text{w}}}h} - 1\right) = -\text{WOU}_{\text{BBL}} \qquad \text{Eq.3}$$

where $C_{\text{w-C}}$ is the concentration of organic matter in the water column; z_{w} is the vertical displacement. Similarly, for pseudo-steady-state consideration, the O_2 flux into the sediment equals the organic carbon flux ($u_{\text{w}} C_{\text{w-C}}^{H}$; $C_{\text{w-C}}^{H}$ is the concentration at the sediment-water interface at depth H) corrected by a recycling efficiency (ε) for not all organic matter reaching sediments being reactive (Li et al., 2012):

$$F_{\text{s-O2}} = -\varepsilon u_{\text{w}} C_{\text{C}}^{H} = -\text{SOU} \qquad \text{Eq.4}$$

Because sedimentation ($u_{\text{w}} C_{\text{C}}^{H}$) is from the leftover of remineralization in the water column:

$$u_{\text{w}} C_{\text{w-C}}^{H} = u_{\text{w}} C_{\text{w-C}}^{H-h} + F_{\text{BBL-O2}} \qquad \text{Eq.5}$$

Combining Eqs.3, 4, and 5,

$$F_{\text{s-O2}} = -\varepsilon u_{\text{w}} C_{\text{w-C}}^{H} = -\varepsilon\left(u_{\text{w}} C_{\text{w-C}}^{H-h} + F_{\text{BBL-O2}}\right) = -\varepsilon u_{\text{w}} C_{\text{w-C}}^{H-h} e^{-\left(\frac{k_{\text{w}}}{u_{\text{w}}}\right)h} \qquad \text{Eq.6}$$

Therefore, from Eqs. 3 and 6,

$$F_{\text{BBL-O2}} = \frac{1}{\varepsilon}\left(e^{\left(\frac{k_{\text{w}}}{u_{\text{w}}}\right)h} - 1\right) F_{\text{s-O2}} = \frac{1}{\varepsilon}\left(e^{fh} - 1\right) F_{\text{s-O2}} \qquad \text{Eq.7.1}$$

$$\text{or } \text{WOU}_{\text{BBL}} = \frac{1}{\varepsilon}\left(e^{fh} - 1\right)\text{SOU} \qquad \text{Eq.7.2}$$

For simplicity, we introduce a parameter, spatial reactivity (f = k_{w}/u_{w}, m^{-1}), which describes the reaction proceeded per-unit distance the particles move downwards. Eq.7.2 shows how WOU_{BBL} and SOU are related (see observations above). We then rewrite the oxygen budget by combining Eq.7 and Eq.2 and integrating it over a period (T), during which the present oxygen level develops:

$$\mathrm{AOU_{BBL}}h = T\left(1+\frac{1}{\varepsilon}\left(e^{fh}-1\right)\right)\mathrm{SOU} \qquad \text{Eq.8}$$

$\mathrm{AOU_{BBL}}$ is the apparent oxygen utilization in the BBL. In summary, oxygen utilization in the BBL is determined by the SOU, the spatial reactivity of organic matter (*f*), the thickness of BBL (*h*), the recycling efficiency in sediments (ε), and the duration (*T*) of stratification to develop the AOU. Similarly, for the whole water column,

$$\mathrm{AOU}\times H = T\left(1+\frac{1}{\varepsilon}\left(e^{fH}-1\right)\right)\mathrm{SOU} \qquad \text{Eq.9}$$

$$\text{and } \mathrm{WOU} = \frac{1}{\varepsilon}\left(e^{fH}-1\right)\mathrm{SOU} \qquad \text{Eq.10}$$

One may fit the data (SOU, *h*, *H*, and AOU) to estimate the parameters (*f*, ε, and *T*). However, as the data is limited and scattered, fitting them to a model with multiple parameters will lead to overfitting producing wrong results. As we are interested in the physical insights rather than definite values (also not realistic as they are naturally variable), we choose to fix the sediment recycling efficiency as ε=0.5, for that the deep sediments bury about half of the organic matter reaching the seafloor (Zhou, 2022), consistent with observations in shallow-oxygenated sediments (Li et al., 2018b). We use *T*=15 days for the lack of information, but also constrained by observations that stratification and hypoxia take two weeks to redevelop after the water column is mixed up (Zhao et al., 2021). Under these constraints, we obtain an organic matter spatial reactivity of *f* =0.026 m^{-1} for the PRE region, and the model reproduces the water column AOU well (Fig.S7). The estimate is consistent with the rate of organic matter remineralization estimated for water depth (*H*) of 10-20 m and that 62% of the organic matter reaches the seafloor: *f*= (1-0.62)/*H*= 0.014-0.028 m^{-1} (details in SI.3).

5. Discussion

5.1 Conditions and time scales for hypoxia— The model explains the relationships between the bottom O_2 level and SOU/*h* in the PRE region and other similar systems (Figs.3c and 3d). The duration of stratification determines the sensitivity of O_2 levels to SOU/*h*: the northern Gulf of Mexico has long periods of stratification (Bianchi et al., 2010; Dzwonkowski et al., 2018) and thus appears more sensitive to SOU: the bottom oxygen drops more with the same level of increase in SOU/*h* (Figs.3a and 3b). This is consistent with model results when the stratification period is set to be longer (e.g., *T*= 30 versus 15 d; Figs.3c and 3d). Alternatively, the high sensitivity of oxygen can be achieved in systems with higher spatial reactivity of settling organic matter (*f*) (Fig.S8).

The model provides several quantitative insights. As expected, $\mathrm{AOU_{BBL}}$ increases with increasing SOU and the effect is more dramatic when BBL is thin (Fig.4a). In the PRE region, a BBL of <10 m is susceptible to hypoxia even at low SOU (Fig.4a). For thicker BBL to reach hypoxia, higher SOU is required, but the effect is not linear: in the PRE region, when SOU is above ~75 mmol m^{-2} d^{-1}, the bottom can easily develop hypoxia regardless of the BBL thickness (Fig.4a). This is because, in environments with

organic matter deposition supporting such high SOU, the WOU would be proportionally high (Eq.7.2).

We can estimate the time required for developing hypoxia (Figs.4b): waters with high SOU and thin BBL become hypoxic within a shorter time. In the PRE region, it requires <~15 days for thin BBLs (<~10 m) to develop hypoxia; the thicker BBLs require longer, but in general not longer than 60 days (Fig.4b). Assuming similar organic matter spatial reactivity (*f*) in other coastal waters (but see discussion later for variability), we can estimate their hypoxia time scales (T_{hyp}; Fig.4c), which can be compared to the stratification time scales to see if hypoxia can develop. For example, in the seasonally hypoxic northern Gulf of Mexico, most hypoxia sites have T_{hyp} of <30-40 days, which is generally shorter than the duration of stratification (30 days to several months) (Bianchi et al., 2010). In the Chesapeake Bay mid-stem central channel, the pycnocline remains stable for several summer months (Boynton et al., 2022), thus hypoxia persistently develops even under low SOU (Fig.4c). More extreme cases are Gulf of St. Lawrence, the Black Sea, and the Baltic Sea, where persistent and even permanent stratification sustains thick hypoxia layers under low SOU (Fig.4c).

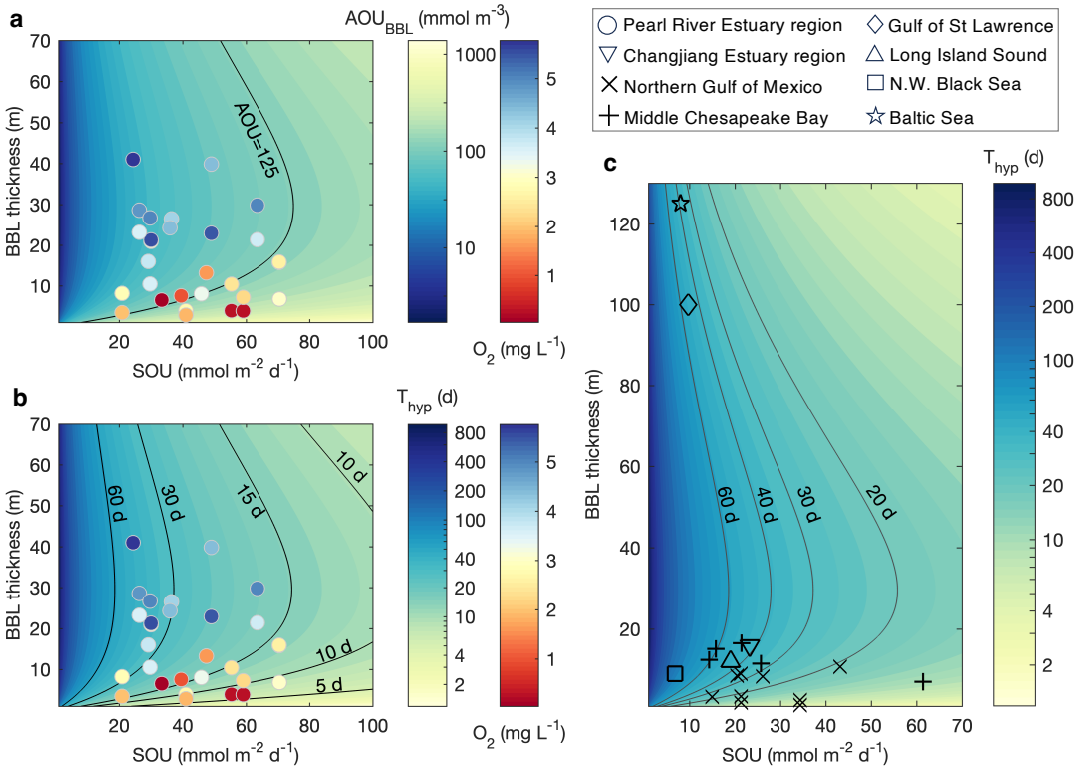

Figure 4 Modeled apparent oxygen utilization (AOU) and time scales for developing hypoxia (T_{hyp}). a) *AOU_{BBL} as a function of SOU and BBL thickness in the PRE region (f= 0.026 m^{-1} and T= 15 d). Higher AOU indicates higher oxygen loss and hypoxia occurs when AOU_{BBL} > 125 mmol m^{-3} (observed bottom O_2 levels are shown with filled colors for comparison);* ***b)*** *the time required for the BBL to become hypoxia (T_{hyp}) (f= 0.026 m^{-1}). If*

stratification sustains longer than T_{hyp}, the bottom water becomes hypoxic. The sites with thick BBL and low SOU need a longer time to develop hypoxia thus the oxygen concentrations remain high. ***c****) same as* ***b*** *but hypoxia sites from other estuarine and coastal systems (Table S3)* (Boynton et al., 2019, 2022; Fennel & Testa, 2019; McCarthy et al., 2013; Zhang et al., 2017).

5.2 Sediments vs water column oxygen uptake— The model can estimate the contribution of SOU to total oxygen loss (%SOU) and explain the global observations in estuaries and coasts (Boynton et al., 2018) (Fig.5): %SOU declines exponentially with the water layer thickness (for whole water column or BBL). Intuitively, the organic matter spends more time in thicker waters consuming oxygen before reaching the sediments, thus reducing the %SOU. The model (Eqs.7.2 and 10) formulates this understanding and explains the possible variabilities: %SOU is regulated by the organic matter spatial reactivity (f) and sediment recycling efficiency (ε). In systems with slowly settling particles (low u_w), the large f (k_w/u_w) would lead to low %SOU (Fig.5). In contrast, SOU contributes more when sedimentation is rapid (large u_w and thus small f; Fig.5). Particle settling velocity is controlled by particle concentrations (Archer & Devol, 1992), but more importantly by turbulence intensity, which can either accelerates settling by promoting particle collisions and flocculation (Ruiz et al., 2004) or decrease it by breaking up floc when shear stress is too large (Manning, 2004). In rivers and estuaries, strong turbulence also leads to particle resuspension (Boynton et al., 2018), increasing the time the particles spend in the water column to consume oxygen (Moriaty et al. 2021). This might explain why rivers and estuaries have low %SOU compared to shelves (Fig.5), where the reactivity of organic matter (k_w) is likely similar if not higher because the organic matter is more planktonic-origin. Likewise, low spatial reactivity in shelf waters may be due to higher particle settling velocity for reasons we can only speculate: salinity increase (Abolfazli & Strom, 2023) and blooming of typically dominated elongated or chains-forming phytoplankton species can promote flocculation and fast settling (Arguedas-Leiva et al., 2022). Sediment recycling efficiency regulates %SOC but to a lesser extent (the shaded area in Fig.5), and the effect becomes smaller when the organic matter spatial reactivity is high (see variability in the width of the shaded area in Fig. 5), as there is less organic matter reaching the sediment for recycling efficiency to make a difference.

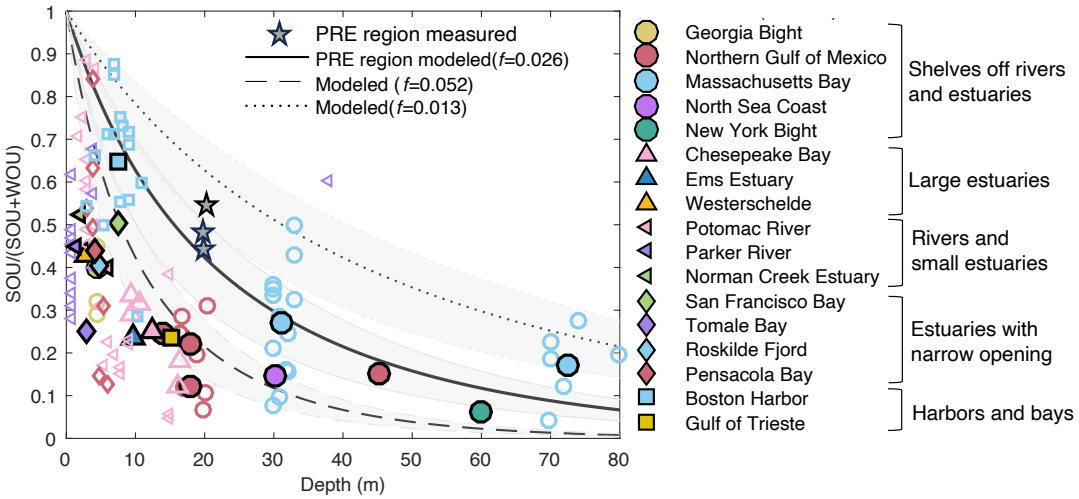

Figure 5 *The contributions of SOU to total oxygen uptake (SOU +WOU) as a function of water layer thickness (for the entire water column or BBL). The solid line represents model results for the PRE region (ε = 0.5; f= 0.026). Results obtained using different spatial reactivities (f) are shown in dotted and dashed lines; shaded areas show variability with different sediment recycling efficiency (ε = 0.3-0.75). Literature data are from* (Boynton et al., 2018; Chi et al., 2021; Kemp et al., 1992; Murrell & Lehrter, 2011)*. Solid markers indicate average values and the open markers of the corresponding colors are individual measurements.*

6. Summary, caveats, and outlooks

Using data in the PRE region, we construct and test a simple mass balance model to understand bottom hypoxia in coastal waters. The model describes oxygen utilization in the BBL due to the sediment and water oxygen uptake (Eqs.8 and 9). While SOU needs to be measured, we show that bottom oxygen levels and water-column stratification can be used to parameterize SOU and increase the data size (Fig.3). WOU is linked to SOU in the model via their intrinsic mass-balance connection (Eqs.7.2 and 10). Therefore, by having data on the water column physical and oxygen conditions across a region (easily obtained from CTD) and some estimates of SOU, the model can estimate other determinants of oxygen loss and quantitatively describe the conditions and time scales for hypoxia formation, as well as the contributions from water column versus sediments.

There are several caveats to using the model. It should be used within areas with similar particle settling velocity and organic matter reactivity. These parameters can vary significantly across regions. Ideally, parameters can be chosen or fitted more locally (e.g., differentiating the inner estuary and the offshore shelf). Moreover, SOU is assumed to be stable during the development of the observed oxygen level, but SOU can decrease when oxygen becomes very limited (<1.5–3.2 mg L^{-1}) (Chi et al., 2021; Murrell

& Lehrter, 2011; Rowe et al., 2002). Therefore, for the model to work, SOU might need to be measured under sufficient overlying-water oxygen (reaction not limited by oxygen) at sites with very low oxygen levels. Other complications of the physical conditions need to be considered, for example, when stratification is disrupted by a typhoon. Despite these limitations, the model provides intuitive and quantitative estimates of hypoxia and can be used to understand the variability among systems and changes under future scenarios (e.g., longer stratification under climate change). The model can also help estimate key constraints, such as the reactivity and settling velocity of particles, to support other mechanistic models.

Acknowledgment

The work is substantially supported by grants from the Research Grant Council (RGC) of the Hong Kong Special Administrative Region, China (Project Reference Numbers: 16303022 and 26305621 to JL, a grant from the National Natural Science Foundation of China to LY (Project No. 42206160), and grants from RGC to JG and LY (Project Reference Numbers: 16307423 and AoE/P-601/23-N to JG). The work is also funded by the Center for Ocean Research in Hong Kong and Macau (CORE). CORE is a joint research center for ocean research between Laoshan Laboratory and Technology and the Hong Kong University of Science and Technology (HKUST). We thank the captain and crew of the R/V *Haike 68* and Chief Scientists Zhongming Lu and Isaac Cheung for assisting in sample collection. Lei Zhou is acknowledged for assistance in sediment sample collection and field analysis. We thank Mark J. McCarthy (Estonian University of Life Sciences) and Wayne S. Gardner (University of Texas at Austin) for providing CTD data from the Northern Gulf of Mexico. These data were collected aboard the R/V Pelican (Louisiana University Marine Consortium) supported by the NOAA/CSCOR Grant (#NA07NOS4780225) to Wayne Gardner. We thank Weicong Cheng and Dou Li for their technical and intellectual support.

Author contributions:

Conceptualization: Jiying Li
Investigation: Jing Sun, Jiying Li, and Xingyu Yang
Data curation: Jing Sun, Jiying Li, and Xingyu Yang
Formal analysis: Jing Sun, Jiying Li, and Liuqian Yu
Methodology: Jing Sun, Jiying Li, Liuqian Yu, and Jianping Gan
Funding acquisition: Jiying Li, Liuqian Yu, and Jianping Gan
Project administration: Jiying Li and Jianping Gan
Supervision: Jiying Li
Writing—original draft: Jing Sun and Jiying Li
Writing—review& editing: Jiying Li, Liuqian Yu, Hongbin Yin, and Jianping Gan

Data Availability Statement

Data presented in the paper are available at DataSpace@HKUST via doi:10.14711/dataset/KCLUQW (Li et al. 2024). Data from the Changjiang estuary region are from Zhang et al. 2017 and Chi et al. 2021; Data from the Northern Gulf of Mexico are from McCarthy et al. 2013; Data from the Chesapeake Bay are from Boynton et al. (2018), Boynton et al. (2022), Boynton and Ceballos (2019), Kemp et al. (1992), and the Chesapeake Bay Program Datahub (https://datahub.chesapeakebay.net). Additional data from other systems are also compiled in Fennel and Testa (2019), Boynton et al. (2018), Boynton et al. (2022), and Kemp et al. (1992).

References

Abolfazli, E., & Strom, K. (2023). Salinity Impacts on Floc Size and Growth Rate With and Without Natural Organic Matter. *Journal of Geophysical Research: Oceans*, *128*(7). https://doi.org/10.1029/2022jc019255

Archer, D., & Devol, A. (1992). Benthic oxygen fluxes on the Washington shelf and slope: A comparison of in situ microelectrode and chamber flux measurements. *Limnology and Oceanography*, *37*(3), 614–629. https://doi.org/10.4319/lo.1992.37.3.0614

Arguedas-Leiva, J.-A., Słomka, J., Lalescu, C. C., Stocker, R., & Wilczek, M. (2022). Elongation enhances encounter rates between phytoplankton in turbulence. *Proceedings of the National Academy of Sciences*, *119*(32), e2203191119. https://doi.org/10.1073/pnas.2203191119

Bianchi, T. S., DiMarco, S. F., Cowan, J. H., Hetland, R. D., Chapman, P., Day, J. W., & Allison, M. A. (2010). The science of hypoxia in the Northern Gulf of Mexico: A review. *Science of The Total Environment*, *408*(7), 1471–1484. https://doi.org/10.1016/j.scitotenv.2009.11.047

Bowman, G. T., & Delfino, J. J. (1980). Sediment oxygen demand techniques: A review and comparison of laboratory and in situ systems. *Water Research*, *14*(5), 491–499. https://doi.org/10.1016/0043-1354(80)90215-8

Boynton, Fraser, W. C., & Alejandra, M. (2019). Chesapeake Bay and Maryland Coastal Bays Sediment-Water Oxygen and Nutrient Flux Data Set. *Mendeley Data*, (V1). https://doi.org/10.17632/jpwvc5jytk.1

Boynton, W. R., Ceballos, M. A. C., Bailey, E. M., Hodgkins, C. L. S., Humphrey, J. L., & Testa, J. M. (2018). Oxygen and Nutrient Exchanges at the Sediment-Water Interface: a Global Synthesis and Critique of Estuarine and Coastal Data. *Estuaries and Coasts*, *41*(2), 301–333. https://doi.org/10.1007/s12237-017-0275-5

Boynton, W. R., Ceballos, M. A. C., Hodgkins, C. L. S., Liang, D., & Testa, J. M. (2022). Large-Scale Spatial and Temporal Patterns and Importance of Sediment–Water Oxygen and Nutrient Fluxes in the Chesapeake Bay Region. *Estuaries and Coasts*, 1–20. https://doi.org/10.1007/s12237-022-01127-0

Cai, W.-J., Dai, M., Wang, Y., Zhai, W., Huang, T., Chen, S., et al. (2004). The biogeochemistry of inorganic carbon and nutrients in the Pearl River estuary and the adjacent Northern South China Sea. *Continental Shelf Research*, *24*(12), 1301–1319. https://doi.org/10.1016/j.csr.2004.04.005

Chi, L., Song, X., Ding, Y., Yuan, Y., Wang, W., Cao, X., et al. (2021). Heterogeneity of the sediment oxygen demand and its contribution to the hypoxia off the Changjiang estuary and its adjacent waters. *Marine Pollution Bulletin*, *172*, 112920. https://doi.org/10.1016/j.marpolbul.2021.112920

Diaz, R. J., & Rosenberg, R. (2008). Spreading Dead Zones and Consequences for Marine Ecosystems. *Science*, *321*(5891), 926–929. https://doi.org/10.1126/science.1156401

Dzwonkowski, B., Fournier, S., Reager, J. T., Milroy, S., Park, K., Shiller, A. M., et al. (2018). Tracking sea surface salinity and dissolved oxygen on a river-influenced, seasonally stratified shelf, Mississippi Bight, northern Gulf of Mexico. *Continental Shelf Research*, *169*, 25–33. https://doi.org/10.1016/j.csr.2018.09.009

Fennel, K., & Testa, J. M. (2019). Biogeochemical Controls on Coastal Hypoxia. *Annual Review of Marine Science*, *11*(1), 105–130. https://doi.org/10.1146/annurev-marine-010318-095138

Fennel, K., Laurent, A., Hetland, R., Justić, D., Ko, D. S., Lehrter, J., et al. (2016). Effects of model physics on hypoxia simulations for the northern Gulf of Mexico: A model intercomparison. *Journal of Geophysical Research: Oceans*, *121*(8), 5731–5750. https://doi.org/10.1002/2015jc011577

Glud, R. N. (2008). Oxygen dynamics of marine sediments. *Marine Biology Research*, *4*(4), 243–289. https://doi.org/10.1080/17451000801888726

Grégoire, M., Garçon, V., Garcia, H., Breitburg, D., Isensee, K., Oschlies, A., et al. (2021). A Global Ocean Oxygen Database and Atlas for Assessing and Predicting Deoxygenation and Ocean Health in the Open and Coastal Ocean. *Frontiers in Marine Science*, *8*, 724913. https://doi.org/10.3389/fmars.2021.724913

Katsev, S., Chaillou, G., Sundby, B., & Mucci, A. (2007). Effects of progressive oxygen depletion on sediment diagenesis and fluxes: A model for the lower St. Lawrence River Estuary. *Limnology and Oceanography*, *52*(6), 2555–2568. https://doi.org/10.4319/lo.2007.52.6.2555

Kemp, W., Sampou, P., Garber, J., Turtle, J., & Boynton, W. (1992). Seasonal depletion of oxygen from bottom waters of Chesapeake Bay: roles of benthic and planktonic respiration and physical exchange processes. *Marine Ecology Progress Series*, *85*, 137–152. https://doi.org/10.3354/meps085137

Laurent, A., & Fennel, K. (2017). Modeling Coastal Hypoxia, Numerical Simulations of Patterns, Controls and Effects of Dissolved Oxygen Dynamics, 149–171. https://doi.org/10.1007/978-3-319-54571-4_7

Levin, L. A., Ekau, W., Gooday, A. J., Jorissen, F., Middelburg, J. J., Naqvi, S. W. A., et al. (2009). Effects of natural and human-induced hypoxia on coastal benthos. *Biogeosciences*, *6*(10), 2063–2098. https://doi.org/10.5194/bg-6-2063-2009

Li, D., Gan, J., Hui, R., Liu, Z., Yu, L., Lu, Z., & Dai, M. (2020). Vortex and Biogeochemical Dynamics for the Hypoxia Formation Within the Coastal Transition Zone off the Pearl River Estuary. *Journal of Geophysical Research: Oceans*, *125*(8). https://doi.org/10.1029/2020jc016178

Li, J., & Katsev, S. (2014). Nitrogen cycling in deeply oxygenated sediments: Results in Lake Superior and implications for marine sediments. *Limnology and Oceanography*, *59*(2), 465–481. https://doi.org/10.4319/lo.2014.59.2.0465

Li, J., Crowe, S. A., Miklesh, D., Kistner, M., Canfield, D. E., & Katsev, S. (2012). Carbon mineralization and oxygen dynamics in sediments with deep oxygen penetration, Lake Superior. *Limnology and Oceanography*, *57*(6), 1634–1650. https://doi.org/10.4319/lo.2012.57.6.1634

Li, J., Zhang, Y., & Katsev, S. (2018a). Phosphorus recycling in deeply oxygenated sediments in Lake Superior controlled by organic matter mineralization. *Limnology and Oceanography*, *63*(3), 1372–1385. https://doi.org/10.1002/lno.10778

Li, J., Brown, E. T., Crowe, S. A., & Katsev, S. (2018b). Sediment geochemistry and contributions to carbon and nutrient cycling in a deep meromictic tropical lake: Lake Malawi (East Africa). *Journal of Great Lakes Research*, *44*(6), 1221–1234. https://doi.org/10.1016/j.jglr.2017.12.001

Li, J., Sun, J, Yu, L., Gan, J., & Yang, X. (2024). Sediment oxygen uptake and hypoxia in the Pearl River Estuary Region [Dataset]. DataSpace@HKUST, https://doi:10.14711/dataset/KCLUQW

Manning, A. J. (2004). The Observed Effects of Turbulence on Estuarine Flocculation. *Journal of Coastal Research. Sediment Transport in European Estuarine Environments: Proceedings of the STRAEE Workshop (WINTER 2004):*, (Special Issue No. 41), 90–104. Retrieved from https://www.jstor.org/stable/25736634

McCarthy, M. J., Carini, S. A., Liu, Z., Ostrom, N. E., & Gardner, W. S. (2013). Oxygen consumption in the water column and sediments of the northern Gulf of Mexico hypoxic zone. *Estuarine, Coastal and Shelf Science*, *123*, 46–53. https://doi.org/10.1016/j.ecss.2013.02.019

Middelburg, J. J., & Levin, L. A. (2009). Coastal hypoxia and sediment biogeochemistry. *Biogeosciences*, *6*(7), 1273–1293. https://doi.org/10.5194/bg-6-1273-2009

Moriarty, J. M., Friedrichs, M. A. M., & Harris, C. K. (2021). Seabed Resuspension in the Chesapeake Bay: Implications for Biogeochemical Cycling and Hypoxia. *Estuaries and Coasts*, *44*(1), 103–122. https://doi.org/10.1007/s12237-020-00763-8

Murrell, M. C., & Lehrter, J. C. (2011). Sediment and Lower Water Column Oxygen Consumption in the Seasonally Hypoxic Region of the Louisiana Continental Shelf. *Estuaries and Coasts*, *34*(5), 912–924. https://doi.org/10.1007/s12237-010-9351-9

Peña, M. A., Katsev, S., Oguz, T., & Gilbert, D. (2010). Modeling dissolved oxygen dynamics and hypoxia. *Biogeosciences*, *7*(3), 933–957. https://doi.org/10.5194/bg-7-933-2010

Rowe, G. T., Kaegi, M. E. C., Morse, J. W., Boland, G. S., & Briones, E. G. E. (2002). Sediment community metabolism associated with continental shelf hypoxia, Northern Gulf of Mexico. *Estuaries*, *25*(6), 1097–1106. https://doi.org/10.1007/bf02692207

Ruiz, J., Macías, D., & Peters, F. (2004). Turbulence increases the average settling velocity of phytoplankton cells. *Proceedings of the National Academy of Sciences*, *101*(51), 17720–17724. https://doi.org/10.1073/pnas.0401539101

Testa, J. M., Li, Y., Lee, Y. J., Li, M., Brady, D. C., Toro, D. M. D., & Kemp, W. M. (2017). Modeling Coastal Hypoxia, Numerical Simulations of Patterns, Controls and Effects of Dissolved Oxygen Dynamics, 95–118. https://doi.org/10.1007/978-3-319-54571-4_5

Trowbridge, J. H., & Lentz, S. J. (2018). The Bottom Boundary Layer. *Annual Review of Marine Science*, *10*(1), 397–420. https://doi.org/10.1146/annurev-marine-121916-063351

Wulff, F., & Stigebrandt. A. (1989). A time-dependent budget model for nutrients in the Baltic Sea. *Glob. Biogeochem. Cycles* **3**: 63–78. https://doi:10.1029/gb003i001p00063

Yu, L., Fennel, K., Laurent, A., Murrell, M. C., & Lehrter, J. C. (2015a). Numerical analysis of the primary processes controlling oxygen dynamics on the Louisiana shelf. *Biogeosciences*, *12*(7), 2063–2076. https://doi.org/10.5194/bg-12-2063-2015

Yu, Liuqian, Fennel, K., & Laurent, A. (2015b). A modeling study of physical controls on hypoxia generation in the northern Gulf of Mexico: Physical Controls on Hypoxia. *Journal of Geophysical Research: Oceans*, *120*(7), 5019–5039. https://doi.org/10.1002/2014jc010634

Yu, Liuqian, Gan, J., Dai, M., Hui, C. R., Lu, Z., & Li, D. (2021). Modeling the role of riverine organic matter in hypoxia formation within the coastal transition zone off the Pearl River Estuary. *Limnology and Oceanography*, *66*(2), 452–468. https://doi.org/10.1002/lno.11616

Zhang, Haiyan, Zhao, L., Sun, Y., Wang, J., & Wei, H. (2017). Contribution of sediment oxygen demand to hypoxia development off the Changjiang Estuary. *Estuarine, Coastal and Shelf Science*, *192*, 149–157. https://doi.org/10.1016/j.ecss.2017.05.006

Zhang, Heng, & Li, S. (2010). Effects of physical and biochemical processes on the dissolved oxygen budget for the Pearl River Estuary during summer. *Journal of Marine Systems*, *79*(1–2), 65–88. https://doi.org/10.1016/j.jmarsys.2009.07.002

Zhao, Y., Uthaipan, K., Lu, Z., Li, Y., Liu, J., Liu, H., et al. (2021). Destruction and reinstatement of coastal hypoxia in the South China Sea off the Pearl River estuary. *Biogeosciences*, *18*(8), 2755–2775. https://doi.org/10.5194/bg-18-2755-2021

Zhou, L. (2022). Sediment oxygen uptake and carbon mineralization in the Pearl River Estuary and adjacent coastal waters. https://doi.org/10.14711/thesis-991013088359403412

Zhu, J., Zhu, Z., Lin, J., Wu, H., & Zhang, J. (2016). Distribution of hypoxia and pycnocline off the Changjiang Estuary, China. *Journal of Marine Systems*, *154*, 28–40. https://doi.org/10.1016/j.jmarsys.2015.05.002

References From the Supporting Information

APHA (1998) Standard Methods for the Examination of Water and Wastewater. 20th Edition, American Public Health Association, American Water Works Association and Water Environmental Federation, Washington DC.

Boynton, W. R., Ceballos, M. A. C., Hodgkins, C. L. S., Liang, D., & Testa, J. M. (2022). Large-Scale Spatial and Temporal Patterns and Importance of Sediment–Water Oxygen and Nutrient Fluxes in the Chesapeake Bay Region. *Estuaries and Coasts*, 1–20. https://doi.org/10.1007/s12237-022-01127-0

Cai, W. J., Dai, M., Wang, Y., Zhai, W., Huang, T., Chen, S., et al. (2004). The biogeochemistry of inorganic carbon and nutrients in the Pearl River estuary and the adjacent Northern South

552 China Sea. *Continental Shelf Research*, *24*(12), 1301–1319.
553 https://doi.org/10.1016/j.csr.2004.04.005
554 Cannaby, H., Fach, B. A., Arkin, S. S., & Salihoglu, B. (2015). Climatic controls on biophysical
555 interactions in the Black Sea under present day conditions and a potential future (A1B) climate
556 scenario. *Journal of Marine Systems*, *141*, 149–166.
557 https://doi.org/10.1016/j.jmarsys.2014.08.005
558 Capet, A., Beckers, J.-M., & Grégoire, M. (2013). Drivers, mechanisms and long-term variability
559 of seasonal hypoxia on the Black Sea northwestern shelf – is there any recovery after
560 eutrophication? *Biogeosciences*, *10*(6), 3943–3962. https://doi.org/10.5194/bg-10-3943-2013
561 Capet, Arthur, Meysman, F. J. R., Akoumianaki, I., Soetaert, K., & Grégoire, M. (2016).
562 Integrating sediment biogeochemistry into 3D oceanic models: A study of benthic-pelagic
563 coupling in the Black Sea. *Ocean Modelling*, *101*, 83–100.
564 https://doi.org/10.1016/j.ocemod.2016.03.006
565 Fennel, K., & Testa, J. M. (2019). Biogeochemical Controls on Coastal Hypoxia. *Annual Review*
566 *of Marine Science*. Retrieved from https://doi.org/10.1146/annurev-marine-010318-095138
567 Glud, R. N. (2008). Oxygen dynamics of marine sediments. *Marine Biology Research*, *4*(4), 243–
568 289. https://doi.org/10.1080/17451000801888726
569 Jørgensen, B. B., & Revsbech, N. P. (1985). Diffusive boundary layers and the oxygen uptake of
570 sediments and detritus1. *Limnology and Oceanography*, *30*(1), 111–122.
571 https://doi.org/10.4319/lo.1985.30.1.0111
572 Lehmann, M. F., Barnett, B., Gélinas, Y., Gilbert, D., Maranger, R. J., Mucci, A., et al. (2009).
573 Aerobic respiration and hypoxia in the Lower St. Lawrence Estuary: Stable isotope ratios of
574 dissolved oxygen constrain oxygen sink partitioning. *Limnology and Oceanography*, *54*(6),
575 2157–2169. https://doi.org/10.4319/lo.2009.54.6.2157
576 Li, J., Crowe, S. A., Miklesh, D., Kistner, M., Canfield, D. E., & Katsev, S. (2012). Carbon
577 mineralization and oxygen dynamics in sediments with deep oxygen penetration, Lake
578 Superior. *Limnology and Oceanography*, *57*(6), 1634–1650.
579 https://doi.org/10.4319/lo.2012.57.6.1634
580 McCarthy, M. J., Carini, S. A., Liu, Z., Ostrom, N. E., & Gardner, W. S. (2013a). Oxygen
581 consumption in the water column and sediments of the northern Gulf of Mexico hypoxic zone.
582 *Estuarine, Coastal and Shelf Science*, *123*, 46–53. https://doi.org/10.1016/j.ecss.2013.02.019
583 McCarthy, M. J., Carini, S. A., Liu, Z., Ostrom, N. E., & Gardner, W. S. (2013b). Oxygen
584 consumption in the water column and sediments of the northern Gulf of Mexico hypoxic zone.
585 *Estuarine, Coastal and Shelf Science*, *123*, 46–53. https://doi.org/10.1016/j.ecss.2013.02.019
586 McDougall, T. J., & Barker, P. M. (2011). *Getting started with TEOS-10 and the Gibbs Seawater*
587 *(GSW) Oceanographic Toolbox* (Vol. SCOR/IAPSO WG127). SCOR/IAPSO WG127.
588 Middelburg, J. J. (1989). A simple rate model for organic matter decomposition in marine
589 sediments. *Geochimica et Cosmochimica Acta*, *53*(7), 1577–1581.
590 https://doi.org/10.1016/0016-7037(89)90239-1
591 Noffke, A., Sommer, S., Dale, A. W., Hall, P. O. J., & Pfannkuche, O. (2016). Benthic nutrient
592 fluxes in the Eastern Gotland Basin (Baltic Sea) with particular focus on microbial mat

ecosystems. *Journal of Marine Systems*, *158*, 1–12. https://doi.org/10.1016/j.jmarsys.2016.01.007

Welsh, B. L., & Eller, F. C. (1991). Mechanisms controlling summertime oxygen depletion in western Long Island Sound. *Estuaries*, *14*(3), 265–278. https://doi.org/10.2307/1351661

Wulff, F., & Stigebrandt, A. (1989). A time-dependent budget model for nutrients in the Baltic Sea. *Global Biogeochemical Cycles*, *3*(1), 63–78. https://doi.org/10.1029/gb003i001p00063

Zhang, H., Zhao, L., Sun, Y., Wang, J., & Wei, H. (2017). Contribution of sediment oxygen demand to hypoxia development off the Changjiang Estuary. *Estuarine, Coastal and Shelf Science*, *192*, 149–157. https://doi.org/10.1016/j.ecss.2017.05.006

Zhou, L. (2022). *Sediment oxygen uptake and carbon mineralization in the Pearl River Estuary and adjacent coastal waters*. Master's Thesis, The Hong Kong University of Science and Technology. doi: 10.14711/thesis-991013088359403412.